RESEARCH ARTICLE

VOLCANICA

# Effects of vent-sourced external water on volcanic column height and collapse

Edgar L. Carrillo *[αβγ], Kristen E. Fauria[β], Tushar Mittal[δ], and Larry G. Mastin[ε]

[α] Department of Physics, Fisk University, Nashville, TN 37208, USA.
[β] Department of Earth and Environmental Science, Vanderbilt University, Nashville, TN 37235, USA.
[γ] Department of Earth Science, University of Oregon, Eugene, OR 97403, USA.
[δ] Department of Geoscience, Pennsylvania State University, University Park, PA 16802, USA.
[ε] U.S. Geological Survey, Cascades Volcano Observatory, Vancouver, WA 98683, USA.

Submitted: 2025-02-19 | Accepted: 2026-02-03 | Published: 2026-02-11

Editor: S. Scollo & A. H. Graettinger | Typesetter: J. Farquharson

## Abstract

Volcanic plumes are important because they spread volcanic material, can impact climate, and pose hazards to aviation. Among eruption processes, column collapse is arguably the most consequential in terms of direct impacts, as it marks the onset of ground-hugging pyroclastic density currents that pose the greatest immediate threat to life and infrastructure. This study investigates how external water, such as is incorporated during subaqueous eruptions, affects the critical condition (including mass eruption rate, temperature, and gas fraction) at which column collapse occurs in the atmosphere, referred to as "the column collapse condition". We use the 1-D plume model, `Plumeria`, to explore how variations in external water (0–60 wt.%), vent exit velocity (75–125 m $s^{-1}$), and initial magma temperature (700–1100 °C) affect the column collapse condition. We find that the occurrence of column collapse is highly sensitive to the amount of external water. Small amounts of external water ($\lesssim$ 25 wt.%) suppress column collapse, whereas higher amounts of water encourage collapse. Using more than 150,000 simulations, we map out the highly non-linear shape of the column collapse condition as a function of mass eruption rates and external water contents. The Richardson number, the ratio of buoyancy to shear forces, offers a useful framework for defining the column collapse condition for eruptions involving external water. This work enhances our understanding of how external water ingestion affects volcanic plume dynamics, including height and column collapse conditions. Recent shallow submarine eruptions that produced very tall atmospheric plumes and partial column collapse (e.g. the 2021 Fukutoku-Oka-no-Ba eruption in Japan and the 2022 Hunga eruption in Tonga) demonstrate the importance of understanding how external water influences the collapse of eruption columns.

Keywords: Volcanic plumes; Column collapse; External water; Plume height; Mass Eruption Rate.

## 1 Introduction

Volcanic eruption columns are turbulent mixtures of tephra, water, and gas that are formed during explosive eruptions. The height of volcanic columns is crucial to determine environmental impacts, such as ash dispersal patterns that affect air travel and the fate of volcanic aerosols that have globally significant climate impacts [McCormick et al. 1995; Carey and Bursik 2015; Vömel et al. 2022]. However, volcanic eruption columns do not always become buoyant and can collapse to form hazardous pyroclastic currents [Koyaguchi and Woods 1996; Sparks et al. 1997; Kaminski and Jaupart 2001; Fagents et al. 2012; Carey and Bursik 2015]. The condition that defines the transition between buoyant plume formation and column collapse is therefore of great importance and is referred to as the "column collapse condition" [Sparks and Wilson 1976; Suzuki and Koyaguchi 2012].

In this study, we focus on the effect of external water introduced near the vent, such as from the ocean, lake, or groundwater, on the column collapse condition and, to a lesser degree, the maximum height of volcanic eruption columns. During an eruption, ejected mixtures of volcanic gas and pyroclasts are generally denser than the surrounding atmosphere (Figure 1A). The mixture is driven upwards by momentum. Once the initial momentum is exhausted, the mixture will only continue to rise and form a buoyant plume if entrainment and heating of air have made the mixture less dense than the atmosphere. Otherwise, the column will collapse. Incorporating external water near the vent may influence the above processes partly because external water changes the column's initial ratio of thermodynamic phases (rock and fluid) and temperature.

Plume height generally increases with mass eruption rate (MER) until column collapse occurs (Figure 1B). A partial collapse occurs when a jet splits into a buoyant plume and a denser component, leading to the formation of pyroclastic density currents [Carazzo et al. 2015]. Three-dimensional (3-D) simulations have further shown that partial collapse can represent a distinct dynamical regime between sustained and fully collapsing columns [Koyaguchi et al. 2018; Trolese et al. 2019]. Eruption columns are more likely to undergo full collapse at high mass eruption rates, as their large diameters inhibit adequate air entrainment into the column interior [Kaminski and Jaupart 2001]. We focus on the influence of external water on the full-collapse transition because the full-collapse threshold governs whether eruptions produce sustained buoyant plumes or collapse into pyroclastic density currents, and it is the regime most appropriately represented by a one-dimensional (1-D) steady-state model.

The ratio of shear to buoyancy forces at the source of the volcanic column, a quantity referred to as the Richardson

* elcar@uoregon.edu

number, is defined as:

$$\mathrm{Ri} = \frac{g' r_v}{u^2}, \tag{1}$$

where $r_v$ is initial vent radius, $u$ is vent exit velocity, $g' = g\,(\rho_{\mathrm{mix}} - \rho_0/\rho_{\mathrm{mix}})$ is reduced gravity, $\rho_{\mathrm{mix}}$ is bulk mixture density at the vent (which is dependent on the magma temperature, gas mass fraction, and external water fraction), $\rho_0$ is the ambient air density, and $g$ is gravitational acceleration. The Richardson number ( Equation 1) has previously been demonstrated to be critical for determining the column collapse condition [Valentine and Wohletz 1989; Suzuki and Koyaguchi 2012]. Several studies support a critical Richardson number of $\mathcal{O}(1)$ defining the column collapse condition [Woods and Caulfield 1992; Suzuki and Koyaguchi 2012]. Values of $\mathrm{Ri} \gtrsim 1$ favor column collapse, whereas $\mathrm{Ri} \lesssim 1$ favor transition to buoyant plume rise. A collapse criterion based on a critical erupted mass fraction has also been proposed [Koyaguchi and Suzuki 2018], but because it is derived for eruption mixtures without external water, the Richardson-number framework is adopted here.

Alternatively, the condition for column collapse has been defined [Degruyter and Bonadonna 2013] by modifying the Richardson number with an entrainment coefficient, $\alpha$, such that

$$\gamma = \frac{\mathrm{Ri}}{\alpha}. \tag{2}$$

Entrainment of ambient fluid into the column can be parameterized as proportional to the plume velocity through the coefficient $\alpha$. The nondimensional parameter $\gamma$ ( Equation 2) compares the characteristic length scale over which jet momentum decays ($\sim 1/\mathrm{Ri}$) with the length scale for entrainment of ambient air into the column ($\sim 1/\alpha$) [Woods and Caulfield 1992; Degruyter and Bonadonna 2013]. When $\gamma > 1$, momentum decays before sufficient entrainment occurs, leading to column collapse; when $\gamma < 1$, entrainment dominates, allowing the column to transition to a buoyant plume. In momentum-dominated regions, entrainment can be expressed as $u_e = \alpha u_z \sqrt{\rho/\rho_{\mathrm{amb}}}$, where $u_z$ is the mean vertical column velocity, $u_e$ is the entrainment velocity normal to the plume, $\rho$ is the column density, and $\rho_{\mathrm{amb}}$ is the ambient atmospheric density (Figure 1A). In buoyancy-dominated regions, this relation simplifies to $u_e = \alpha u_z$ [Woods 1988; Mastin 2007].

Quantitative consideration of the column collapse condition largely neglects the role of external water, which matters because a significant fraction of eruptions occur through water [White et al. 2003]. Large amounts of external water can promote column collapse by reducing the efficiency of ambient fluid entrainment necessary for maintaining buoyant plume ascent [Sheridan and Wohletz 1983]. Modeling work in Koyaguchi and Woods [1996] demonstrated that external water fractions above ≈20 wt.% promote column collapse and the formation of dense, wet, and cold mixtures. Mastin [2007] generally agreed with these findings, although they predicted column collapse at lower MER for given water contents. Two-dimensional (2-D) simulations have built upon this 1-D work and demonstrated that column collapse is a complicated dynamical process and that partial collapse is possible [Van Eaton et al. 2012a].

To date, the variation in column collapse with external water content has only been qualitatively known [Koyaguchi and Woods 1996]. In this study, we conduct over 150,000 simulations with the 1-D model `Plumeria` (U.S. Geological Survey software; Mastin 2007; 2014; 2024) to systematically define the column collapse condition as a function of external water content, mass eruption rate, magma temperature, and exit velocity. Because `Plumeria` is a 1-D steady-state model, we cannot investigate the mechanics of partial collapse and pyroclastic current formation, which have been explored using 3-D approaches [Koyaguchi et al. 2018; Trolese et al. 2019]. Instead, our large ensemble of simulations enables us to systematically examine how external water influences the conditions for full column collapse. We also compare our plume height results to scaling-based models for plume height, $H \propto Q^{0.25}$, where $H$ is plume height and $Q$ is eruption mass flux [Morton et al. 1956; Sparks et al. 1997], (Figure 1B). This comparison reveals that external water primarily influences the column collapse condition, with only a minimal impact on maximum plume heights. Overall, we clarify how external water interacts with eruption parameters to influence the likelihood of column collapse.

## 2 Methods

### 2.1 Plume model

We used `Plumeria`, a 1-D steady-state volcanic plume model, to examine the effects of external water on the column collapse condition and maximum height of sustained eruption columns (Figure 2 and Figure 3A). `Plumeria` calculates the column's velocity, entrainment rate, temperature, density, mass fraction of air, volcanic particles, and water (in vapor, liquid, and ice forms) as functions of height, while conserving momentum, mass, and total energy along the vertical path of the column. Importantly, `Plumeria` accounts for the thermodynamic effects of phase changes, including the impact of water condensation and ice formation, on column dynamics. The governing equations for these processes are presented in detail by Mastin [2007, 2014], and we refer readers there for the full formulation.

To further examine column stability, we track the evolution of column velocity ($u_z$), mixture temperature ($T_{\mathrm{mix}}$), and mixture density ($\rho_m$) to understand the mechanisms influencing column collapse and column height (Figure 3B–3G). Although `Plumeria` allows for atmospheric moisture entrainment along the plume, we assume that all external water is entrained at the vent, where it is well mixed with magma and magmatic gas (blue box in Figure 1A), and thus neglect atmospheric humidity. Additionally, we do not consider the effects of wind, tephra fallout, and ash aggregation.

### 2.2 Initial conditions

To clarify how `Plumeria` is initialized, we define the starting location and thermodynamic state of the erupting mixture prior to entry into the atmospheric column. Following Woods [1995] and the assumptions described in Supplementary Material Section S2, we initialize the model at the point just above the vent where the decompressing jet has fully equilibrated

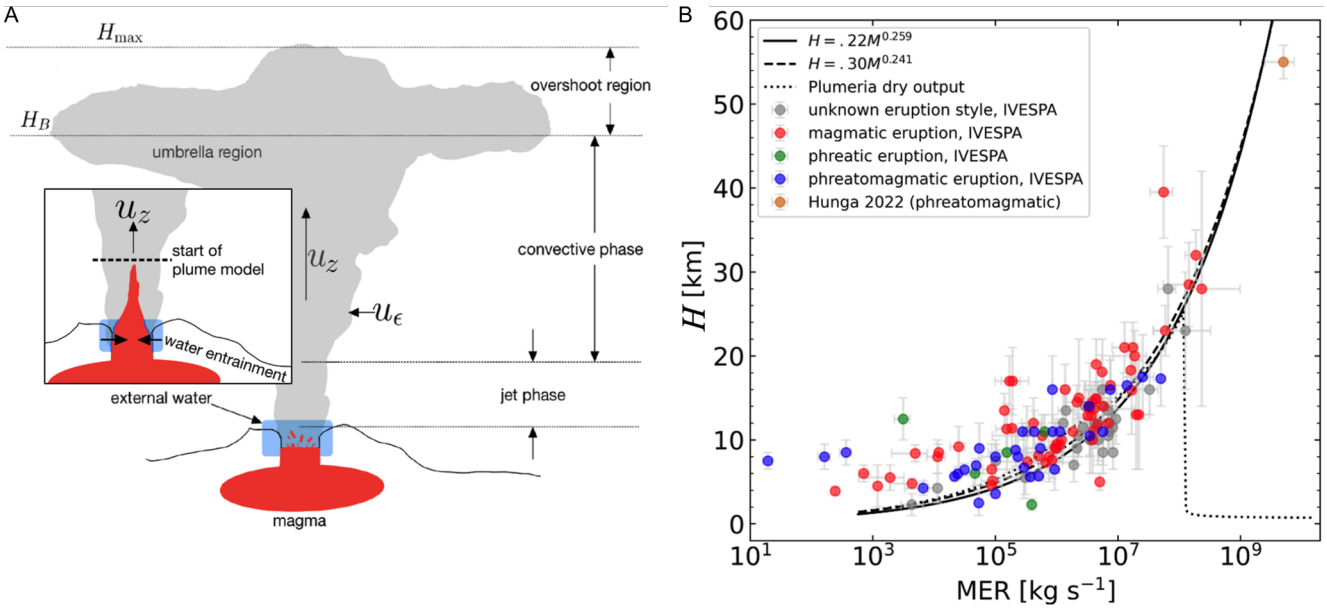


Figure 1: [A] Conceptual model of a volcanic plume. The maximum height of the volcanic plume is $H_{max}$ (includes overshoot region), the neutral buoyancy height is $H_B$ (height of umbrella region), the plume velocity is categorized by a single value, $u_z$ (but varies along the plume axis), and the entrainment velocity is $u_\epsilon$. The blue box at the vent indicates an external water source. The inset illustrates the near-vent region, showing jet expansion, external water entrainment along the margins, and the level at which the plume model is initialized ("start of plume model"). Note that the "start of plume model" in the inset marks the pressure-equilibrated initialization level and is not the same as the jet–plume transition height indicated in the main schematic. [B] Mass eruption rate (MER) versus plume height ($H$). We plot observational eruption data from the Independent Volcanic Eruption Source Parameter Archive (IVESPA)[Aubry et al. 2021] and for the 15 Jan 2022 Hunga eruption [Carr et al. 2022; Proud et al. 2022; Van Eaton et al. 2023]. We show empirical relations between $H$ (km) and erupted mass flux ($M$, kg s$^{-1}$) from Sparks et al. [1997] ($H = 0.22M^{0.259}$) and Mastin et al. [2009] ($H = 0.30M^{0.241}$), both converted to mass flux from volume flux using Equations 1 and 2 from Mastin [2014]. We also show model maximum plume heights ($H_{\mathrm{max}}$) from a dry `Plumeria` model run (no external water) for a range of MERs ($10^3$–$10^{10}$ kg s$^{-1}$) with an initial exit velocity of 100 m s$^{-1}$. Uncertainties in MER estimates are described in the Supplementary Material (Data Sources and Uncertainty Calculations).

to atmospheric pressure (schematized in Figure 1A inset). At this location, magma and magmatic gas have undergone rapid expansion from a narrow near-vent constriction into a wider jet. The model initiation point is not the same as the jet to convective column transition (Figure 1A).

For dry simulations, the initial mixture properties (velocity, temperature, density, and composition) are computed directly from the chosen magma temperature, magmatic gas content, and exit velocity. For wet simulations, external water that enters the jet below the initialization point is assumed to be fully mixed before the plume model begins; its thermodynamic effects (heating, vaporization, condensation) are internally computed by `Plumeria`.

### 2.3 External water addition

External water is assumed to enter the jet along its margins inside the crater or conduit, at atmospheric pressure, before mixing with the erupting material (Supplementary Material Figure S1). Once added, the water thermally equilibrates with the hot mixture and the bulk density decreases. Additionally, we calculate the "dry equivalent" mass flux, $M_d = M_T(1 - w)$, where $M_d$ is the mass flux (magma+gas) without external water, and $M_T$ includes the mass flux with magma, gas, and external water (Section S1 in the supplementary file).

Holding this flux constant requires adjusting the initial jet geometry: adding water reduces mixture density, so the jet cross-section must increase to maintain the same mass flux. Thus, in wet simulations, we retain the dry-plume exit velocity and increase the effective jet diameter to match the prescribed MER. This choice has a clear physical basis in the near-vent expansion geometry and avoids artificially increasing entrainment by raising velocity. This approach preserves dynamical consistency and allows the wet-dry comparison to isolate the thermodynamic effects of external water.

### 2.4 Model parameters

We used values of external water content ($w$) from 0–60 wt.%, initial magma temperatures ($T_m$) of 700, 900, and 1100 °C, and vent exit velocities ($u$) of 75, 100, and 125 m s$^{-1}$ to assess their impacts on maximum column height and to determine the column collapse conditions for MERs ($M_d$) of $10^2$–$10^{12}$ kg s$^{-1}$ (Figure 2).

For variables held constant, we selected values consistent with Mastin [2007] and Koyaguchi and Woods [1996], representing realistic atmospheric, magmatic, and vent initial conditions for volcanic columns (Table 1). The upper bound of $10^{12}$ kg s$^{-1}$ corresponds to eruption intensities approaching those inferred for the largest known explosive eruptions

(VEI 8 [Mason et al. 2004]). Although a single vent could not physically sustain such fluxes, such rates are plausible for broad, fissure-fed, or multi-vent systems whose individual plumes merge to form a single, coherent column at the base of the atmosphere. Accordingly, the vent "diameter" used in the scaling should be interpreted as an effective source width, corresponding to the diameter of the mixed jet at atmospheric equilibration, rather than the physical diameter of any individual vent.

Table 1: Input parameters used for `Plumeria` model runs.

| Parameter | Description | Value |
|---|---|---|
| $T_0^{\mathrm{amb}}$ | Atmospheric temperature at vent (K) | 273 |
| $\frac{dT}{dz}$ | Tropospheric lapse rate (K m$^{-1}$) | −0.065 |
| $\frac{dT^{\mathrm{strat}}}{dz}$ | Stratospheric lapse rate (K m$^{-1}$) | 0.0016 |
| $z^{\mathrm{trop}}$ | Tropopause elevation (m) | 11 000 |
| $H^{\mathrm{trop}}$ | Tropopause thickness* (m) | 9000 |
| $\phi$ | Relative humidity (%) | 0 |
| $m_0$ | Initial magmatic gas mass fraction | 0.03 |
| $T_m$ | Magma temperature (°C) | 700, 900, 1100 |
| $C_m$ | Magma specific heat (J kg$^{-1}$ K$^{-1}$) | 1000 |
| $\rho_m$ | Magma density (DRE†) (kg m$^{-3}$) | 2500 |
| $z_0$ | Vent elevation above sea level (m) | 0 |
| $u$ | Vent exit velocity (m s$^{-1}$) | 75, 100, 125 |
| $w$ | External water mass fraction (wt.%) | 0–60 |
| $d_v$ | Effective vent diameter (m) | 1—~66 000‡ |

* Isothermal layer at base of the stratosphere.
† DRE: dense rock equivalent.
‡ Maximum equivalent source diameter required to achieve a mass eruption rate on the order of $10^{12}$ kg s$^{-1}$.

We note that approximately 0.16 % of the simulations did not converge and were excluded from the final dataset. These non-convergent cases are confined to a very small region of parameter space and reflect numerical difficulties in a subset of stiff regimes of the governing equations. Their exclusion does not affect the large-scale trends discussed here. For visualization purposes only, the remaining data were interpolated in Figure 2 and Figure 3A.

## 3 Model Results

### 3.1 Effects of external water on bulk mixture dynamics

Our simulations show that adding external water alters the eruptive mixture's initial density and temperature. At low water fractions, bulk density decreases as water vaporizes, enhancing buoyancy. However, once ~25 wt.% of water is added, mixture temperatures fall to ~100 °C, producing liquid water in the mixture. This increases bulk density and promotes column collapse. These thresholds reflect simple energy-balance arguments (see Supplementary Material Section S3 and Figure S3 for full derivations and compositional evolution) and help explain the transition between collapse suppression and promotion observed in Figure 2.

### 3.2 Effects of external water on the column collapse condition

We find that external water exerts a strong influence on the column collapse condition. Figure 2 shows maximum column height as a function of external water content, vent exit velocity, initial magma temperature, and MER. The column collapse condition is delineated by the dashed black line and exhibits a consistent form across all nine subplots.

Dry columns collapse at MER values near $10^8$ kg s$^{-1}$ [Carey and Bursik 2015], and small amounts of external water ($< 25 \pm 4$ wt.%) shift the collapse condition to higher MERs. In contrast, external water fractions exceeding ~ 20 % promote column collapse [e.g. Koyaguchi and Woods 1996]. Initial magma temperature and vent exit velocity also modify the collapse condition: higher values of either parameter shift the threshold to higher MERs, meaning that buoyant plumes form more readily under hotter or faster initial conditions. Altogether, Figure 2 shows that the column collapse condition can span three orders of magnitude in MER, is affected by the combined effects of exit velocity and magma temperature, and strongly depends on external water content.

### 3.3 Effects of external water on column height

To explore how external water impacts the column collapse condition, we plot the difference in maximum column height between wet and dry eruptions (Figure 3A),

$$\Delta z = H_{\mathrm{wet}} - H_{\mathrm{dry}}, \tag{3}$$

where $H_{\mathrm{wet}}$ is the modeled maximum column height for an eruption involving external water and $H_{\mathrm{dry}}$ is the maximum column height for an eruption with the same MER, $M_d$, and exit velocity but without external water. We find from Figure 3A, that this differencing clearly highlights the column collapse condition as a function of MER and external water (for $T_m = 900$ °C and $u = 100$ m s$^{-1}$ and with other variables set according to Table 1 parameters).

By plotting $\Delta z$ ( Equation 3), we can visualize the water content conditions that allow columns that otherwise would have become buoyant to collapse (we call this Region 2 in Figure 3A). We also see, in what we label Region 4, that under certain circumstances, buoyant plumes can form due to the incorporation of external water, whereas dry columns would have collapsed. In Region 1, buoyant plumes form, and there is little difference between the height of wet and dry plumes. In Region 3, collapsing columns form because the mixture is too dense to become buoyant, regardless of the amount of water added.

We find that external water has only a limited effect on the height of large, buoyant plumes when they form (Region 1). Across all simulations in this regime, the average change in maximum plume height is a decrease of approximately 48 % relative to the dry cases, with the largest fractional decreases occurring for the smallest plumes. In contrast, the tallest plumes show more modest reductions of approximately 25 %, corresponding to absolute differences on the or-

der of 10 km (e.g. from 40 km to 30 km). Consistent with Koyaguchi and Woods [1996], this limited sensitivity arises because (1) plume height is primarily controlled by thermal energy within the plume, and (2) external water contributes relatively little heat compared to the magma (Supplementary Material Section S5 and Equation S19). Simplified scaling relations such as $H \propto Q^{0.25}$ therefore remain reasonable for wet eruptions that produce buoyant (non-collapsing) plumes. This conclusion specifically applies to vent-sourced external water; background atmospheric humidity, which can enhance plume height through latent-heat release during condensation (see Supplementary Material Section S5), is not included here.

Instead, external water has the primary effect of strongly shifting the column collapse condition. In Figure 3, we show a select number of vertical profiles of column behavior. These profiles help to illustrate how large fractions of additional water can cause column collapse (Region 2, Figure 3B–3D) while modest fractions of water promote buoyant plume formation (Region 4, Figure 3E–3G).

### 3.4 Effects of ice formation on plume height and collapse

We evaluated the influence of ice formation by comparing otherwise identical model runs (using the same input values as in Figure 2E) in which ice formation was either allowed or suppressed (see Supplementary Material Section S6 and Supplementary Material Figure S6). Although latent heat release from freezing has been proposed to enhance plume height [Herzog et al. 1998], we find that its impact is minimal. Allowing ice formation changes the modeled difference in maximum column height between wet and dry eruptions by only approximately 9 % (from 2.90 km to 2.63 km lower than dry eruptions). Moreover, ice does not form at the typical altitudes where column collapse occurs, and thus has no influence on the collapse threshold itself.

Within the constraints of this model, column buoyancy is therefore controlled primarily by magmatic thermal energy and by latent heat released during condensation of water vapor to liquid, with freezing playing a negligible role in plume dynamics and collapse. However, ice formation can still strongly influence ash aggregation and fallout processes [Van Eaton et al. 2012b], which may indirectly affect plume behavior in ways not captured by this steady-state framework.

## 4 Discussion

Figure 2 and Figure 3 show that external water has two different impacts on the column collapse condition. At low water content ($< 25 \pm 4$ wt. %), water acts to promote buoyant plume formation (suppress collapse), while higher water content promotes collapse. The specific amount of external water that defines the trade-off between column collapse suppression and promotion depends on initial magma temperature and exit velocity. The $25 \pm 4$ wt. % value is consistent with previous work [Koyaguchi and Woods 1996]. In addition, $25 \pm 4$ wt. % is the water content at which liquid water starts to form in a mixture between magma and external water (Supplementary Material Section S3.5-3.6, Supplementary Material Figure S3).

### 4.1 Suppression of column collapse with low fractions of external water

Low ($< 25 \pm 4$ wt.%) amounts of external water are known to suppress column collapse [Koyaguchi and Woods 1996; Carey and Bursik 2015; Rowell et al. 2022]. In Region 4 of our simulations (Figure 3), high-MER eruptions ($\gtrsim 10^8$ kg s$^{-1}$) yield wet columns that extend up to 40 km higher than dry analogues that collapse, while the maximum increase across all simulations reaches ~55 km.

The promotion of buoyant plume formation at low external water fractions arises because small to moderate amounts of added water do not cool the eruptive mixture below the boiling temperature. As a result, the mixture remains hot enough that all entrained external water is vaporized, increasing the vapor mass fraction and decreasing bulk density. This additional vapor allows the column to become buoyant with less air entrainment during the jet phase than in the dry case (Figure 3G).

In the context of Equation 2, the addition of external water effectively reduces the characteristic length scale over which ambient fluid must be entrained for the mixture to become buoyant, because the entrained fluid now includes both air and vaporized external water.

Region 4 is thus a “sweet spot” where external water decreases initial mixture density and increases plume height by making an otherwise collapsing column buoyant. This behavior reflects the bifurcation-like nature of the column collapse condition: near the critical point (defined here as the combination of mixture density, momentum, and entrainment efficiency at which the column transitions between buoyant rise and collapse), small changes in initial conditions can produce disproportionately large changes in eruptive outcome.

### 4.2 Promotion of column collapse with large fractions of external water

Column collapse occurs when large fractions of water are added (Region 2) because a large amount of external water makes the initial mixture too cold and too dense to become buoyant. Figure 3C shows that in the dry case, the initial temperature is close to the magmatic temperature, while in the case where 30 wt.% external water is added, the temperature is close to 100 °C (as expected from Supplementary Material Section S3.2). As the mixture temperature approaches the boiling point, water exists in both vapor and liquid states within the column. The liquid water is denser than ambient air, thus reducing the column buoyancy. Furthermore, since the column’s thermal energy is used up to heat/vaporize external water, the entrained ambient air is not heated and expanded as effectively. Therefore, relative to the dry case, we see column collapse because external water heating consumes a substantial portion of the thermal energy available, preventing buoyant plume formation. The mixture thus forms a wet collapsing column.

### 4.3 Comparison to previous findings

Our results build upon those of Koyaguchi and Woods [1996] who found that: 1) small amounts of water decrease mixture

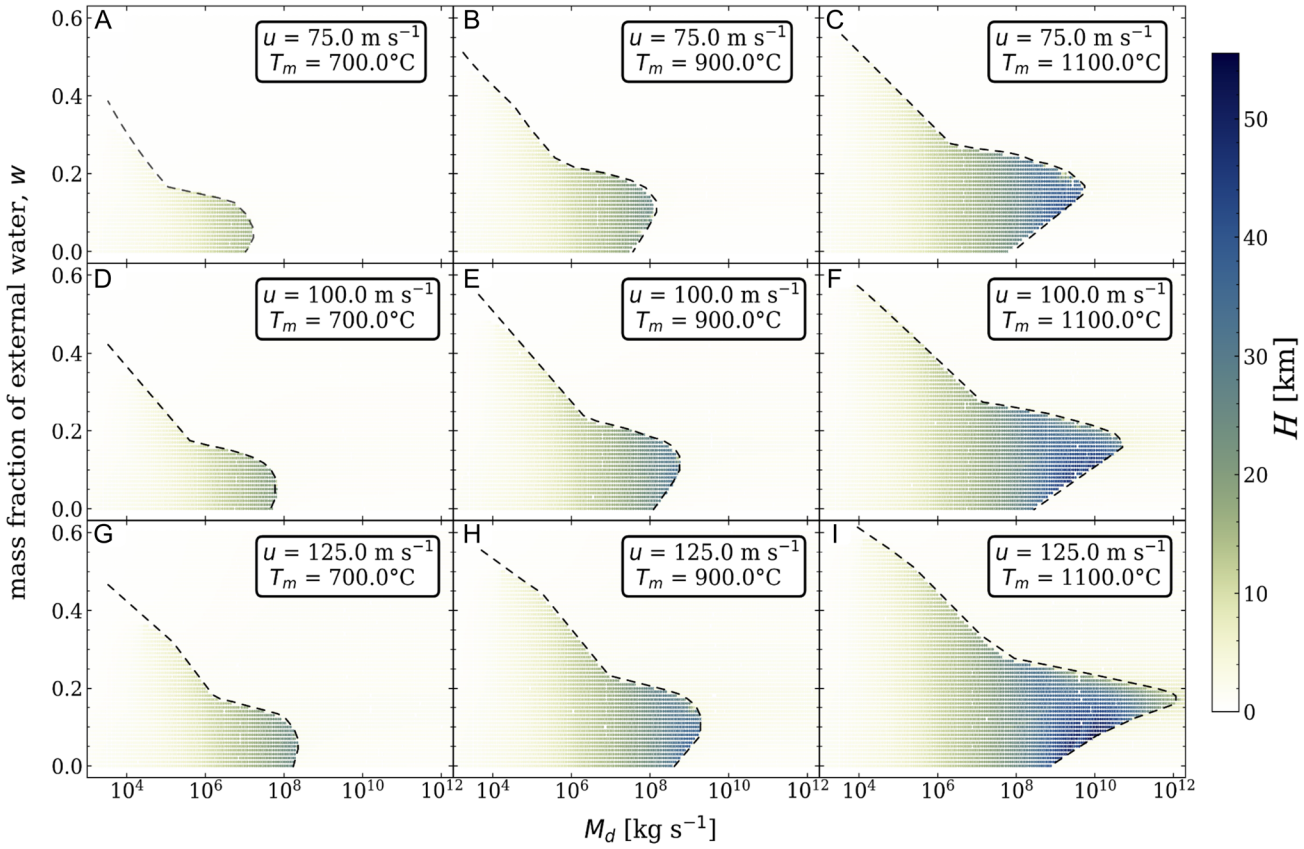


Figure 2: `Plumeria` results for maximum column height ($H$, km) as a function of mass fraction of external water ($w$) and mass eruption rate ($M_d$, kg s$^{-1}$). Panels [A]–[I] show the results of the varying vent exit velocities ($u$) and initial magma temperatures ($T_m$) (see panel annotations). The black dashed lines identify a distinct boundary indicating a mass flux threshold at which buoyant plumes cease to form under varying external water contents (column collapse condition). The columns' initial magma temperature and vent exit velocity affect the column collapse condition's location.

density and thus allow Plinian eruption columns to develop more easily (i.e. at lower initial velocities); 2) large amounts of external water prevent eruption columns from becoming buoyant; and 3) that columns are not significantly affected by external water at low eruption rates (MER $\lesssim 10^8$ kg s$^{-1}$). Our contribution adds, through an extensive parametric study, a comprehensive assessment and visualization of the complex shape of the column collapse condition (Figure 2). In contrast to Koyaguchi and Woods [1996], we hold exit velocity constant as we increase MER by increasing vent diameter. By increasing MER without increasing exit velocity, the eruption columns collapse at lower MER values compared to [Koyaguchi and Woods 1996].

Mastin et al. [2024] explored the effects of external water on plume heights at large mass fluxes. They find that at very high mass fluxes, both wet ($\lessapprox$ 20 wt.%) and dry buoyant plumes can form; however, the wet plumes were lower by up to 40 km (e.g. purple diamonds in Figure 4a of Mastin et al. [2024]). We do not clearly see this behavior in our results. However, we used initial velocities lower than those used by Mastin et al. [2024] (up to 125 m s$^{-1}$ versus 100–300 m s$^{-1}$), which we attribute to the discrepancy. Instead, we find that, at lower initial velocities and MERs, the addition of water does not significantly change plume height; it only affects it by promoting or suppressing column collapse.

### 4.4 Non-dimensional scaling of column collapse

The Richardson number ( Equation 1) has previously been demonstrated to provide an important control on column collapse, partly because 1/Ri expresses the length scale over which the initial jet momentum goes to zero for collapsing columns, whereas in sustained plumes momentum is carried higher into the atmosphere [Woods and Caulfield 1992]. Previously, the column collapse condition has been depicted qualitatively and we expand upon that work by illustrating a quantitative dependence of column collapse on MER and water content (Koyaguchi and Woods 1996; Figure 4A). In Figure 4B, we cast the column collapse conditions from Figure 2 in terms of both Ri and water content ($w$). Large Ri indicates that the plume is initially dominated by negative buoyancy forces, small Ri indicates that momentum (shear) is dominant, and Ri $\approx$ 1 suggests both matter. Figure 4B also shows that positively buoyant plumes form only for Ri $\lessapprox$ 1. This threshold is consistent with the concept that, for buoyant plumes to form, enough shear must occur to produce significant air entrainment, which makes the column buoyant. That said, a Ri $\lessapprox$ 1 threshold is not sufficient to determine the column

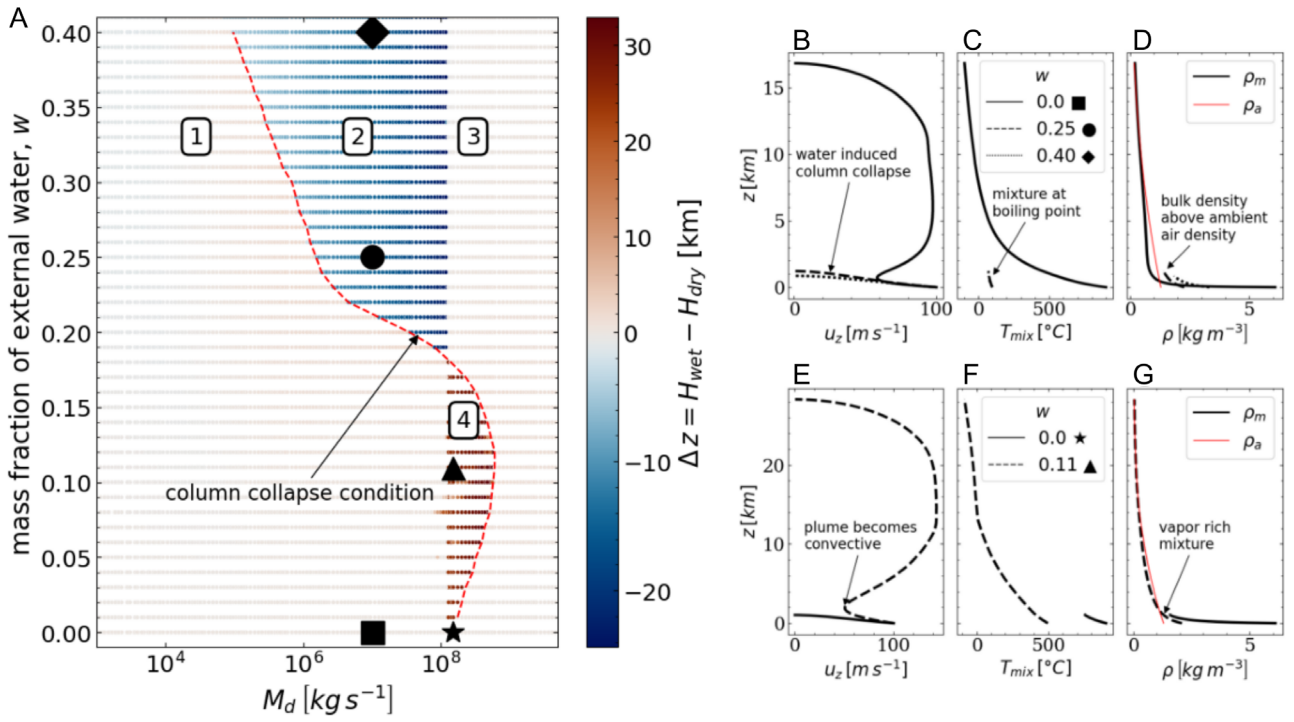


Figure 3: [A] Effect of external water, $w$, on column height difference relative to the dry case ($\Delta z$, km) for various initial mass eruption rates ($M_d$, kg s$^{-1}$) and for the initial conditions corresponding to Figure 2E. The numbers in the squares represent the four collapse-response regimes describing how external water modifies the column collapse condition. The column collapse condition marks the point at which buoyant plumes cease to form. Black symbols denote the initial conditions of the runs shown in panels [B]–[G]: the triangle corresponds to regime 4 (panels [E]–[G]); the circle and diamond correspond to regime 2 (panels [B]–[C]); and the square and star represent the no-water equivalents of regimes 2 and 4. Panels [B]–[G] show results from individual `Plumeria` simulations with initial mass eruption rate values of ~$10^7$ and ~$10^8$ kg s$^{-1}$ in panels [B]–[D] and [E]–[G], respectively. The ambient air density profile is shown for reference in panels [D] and [G].

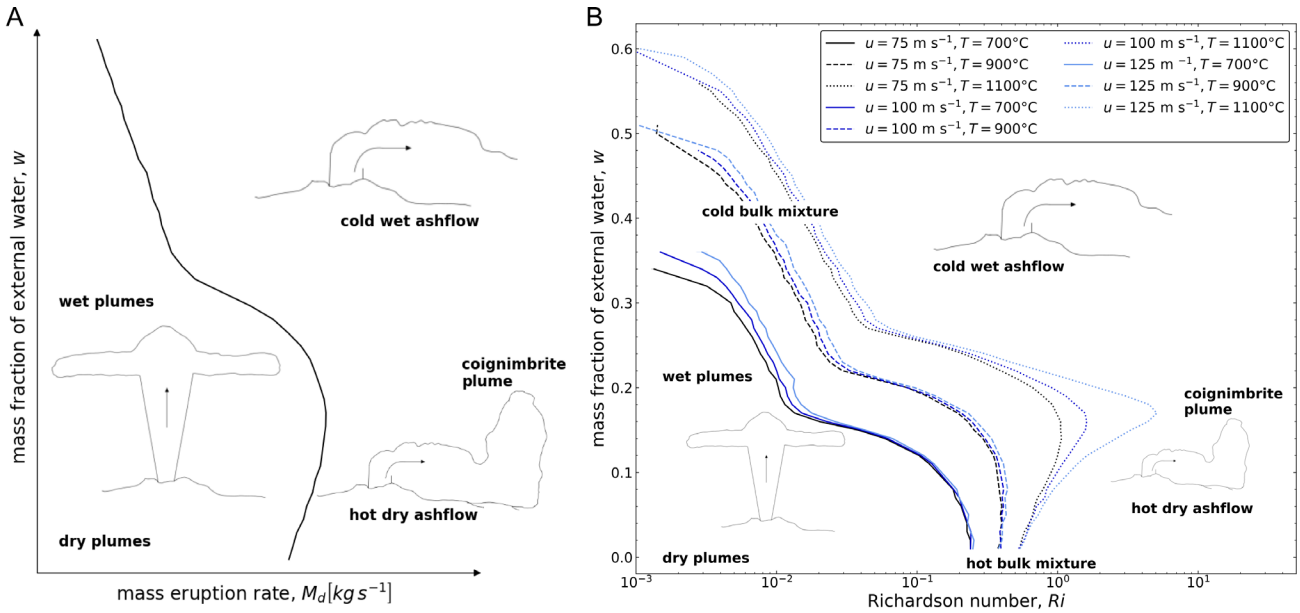


Figure 4: [A] Mixing diagram adapted from Figure 10 in Koyaguchi and Woods [1996] showing the qualitative relation between the mass flux of magma, external water added, and maximum column height. [B] Depiction of the non-dimensional column collapse condition where a wet buoyant plume can form as external water is added to the initial bulk mixture. Based on thresholds from Figure 2.

collapse condition because the dependence of Ri on external water content ($w$) is strongly non-linear.

Figure 4B shows that the dependence of the column collapse condition on velocity goes away when plotted as a function of Ri. We find the magma temperature (and hence $g'$) affects the column collapse condition since it controls the available thermal energy for heating the entrained air. This scaling also suggests that there is a strong tradeoff between the effects of $u$ and $r_v$ in the Richardson Number. That is, as vent exit velocity increases, the critical vent diameter at which column collapse occurs also increases according to $r_v^{\text{critical}} \propto u^2 \text{Ri}_{\text{crit}}$ for a given magma temperature. Since MER $\propto u r_v^2$, the Ri scaling implies that the critical MER at which a column collapses scales as $\text{MER}_{\text{crit}} \propto u^5$ (shown non-dimensionally by Equation 5 in Koyaguchi and Suzuki 2018). This analysis is consistent with the results from our parameter space wherein a change of vent velocity from 75 $\text{m s}^{-1}$ to 125 $\text{m s}^{-1}$ leads to about an order of magnitude increase in the MER associated with the column collapse and rightward shift in the column collapse condition.

An alternative framework to describe column collapse was proposed by Koyaguchi and Suzuki [2018]. In their formulation, the collapse condition is expressed in terms of a critical mass fraction of entrained air required for the mixture to become buoyant; collapse occurs if the eruptive mixture cannot entrain sufficient ambient air before its initial momentum is exhausted. However, the Koyaguchi and Suzuki [2018] critical mass fraction does not incorporate effects from external water. In Supplementary Material Section S8, we expand upon Koyaguchi and Suzuki's critical mass fraction derivation to incorporate external water (Supplementary Material Equation S24). However, our derivation does not fully account for effects from phase changes (liquid to vapor), and thus we compare our results to the Richardson number ( Equation 1).

Overall, Figure 4 shows how variable amounts of external water shift the column collapse condition and how the column collapse condition relates to general eruptive behavior. Although we show that the column collapse condition is a complex function of w, MER, and initial temperature, Ri $\lessapprox 1$ and $w < 25 \pm 4$ wt.% water delineate the phase space in which buoyant plumes most readily form.

### 4.5 Model limitations

One-dimensional models like `Plumeria` can determine the conditions that produce column collapse in a sustained eruption, but do not detail the collapse process, partial collapses, or the complex instabilities within a volcanic plume. These models often rely on empirical parameters, such as entrainment coefficients, to parameterize complex small-scale fluid instabilities, and this can limit their accuracy [Mastin 2007]. However, they have proven effective in predicting column height relatively well and offer the advantage of reduced computational demands, enabling numerous simulations [Costa et al. 2016].

In contrast, three-dimensional models capture the spatial and temporal variations within the volcanic column, including changes in concentration, temperature, pressure, and velocity, all of which can influence buoyancy [Costa et al. 2016; Suzuki et al. 2016]. These models can directly simulate air entrainment dynamics and account for umbrella-region effects, partial column collapse scenarios, plume-ash microphysics, and the formation of pyroclastic density currents [Van Eaton et al. 2012a; Suzuki et al. 2016]. However, simulating fully sustained columns with 3-D models is computationally demanding: high near-vent velocities often require small time steps, grid spacing can be large relative to the eruption column, and sub-grid turbulence must be parameterized. Thus, while 3-D models provide critical insight into processes not captured in 1-D, exploring how these dynamics influence the collapse condition remains a challenge, particularly during large eruptions, especially when additional complexities such as phase changes between water vapor, liquid, and ice further alter entrainment and buoyancy [Van Eaton et al. 2012a; Ichihara et al. 2023].

Additionally, we treat the external water mass fraction ($w$) as a free parameter in this study and focus only on the eruption column after the jet has decompressed to atmospheric pressure. The model does not resolve the dynamics of magma-water heat transfer, fragmentation, or near-vent entrainment, all of which are known to influence $w$ [Fagents et al. 2012; Rowell et al. 2022]. These processes are important because magma–water interaction modifies jet properties and enhances ash fragmentation [Wohletz 1986; Fagents et al. 2012; Cahalan and Dufek 2021; Rowell et al. 2022].

Rowell et al. [2022] used a coupled magma-water interaction model to examine water entrainment and quench fragmentation processes as a jet rises through the water column. Their results highlight the complexity of wet eruptions prior to column formation in air. In particular, they show that the mass fraction of external water entrained into the mixture is strongly dependent on vent water depth. Although the collapse regime they investigate applies to the jet within the water column, their findings provide useful constraints on the range of $w$ values that may feed the subaerial column; in their simulations, external water contents can exceed 30 wt.% at shallow water depths.

### 4.6 Recent examples of water-rich eruptions

Recent large and shallow submarine eruptions highlight both the importance and challenges associated with wet volcanic eruption column dynamics. The January 15, 2022, Hunga eruption produced a record-breaking 55 km atmospheric plume [Proud et al. 2022] and increased stratospheric water load by 10 % in 2022 [Vömel et al. 2022]. The height of the water-rich Hunga plume may have been impacted by the phreatomagmatic nature of the eruption [Gupta et al. 2022; Vömel et al. 2022; Xu et al. 2022]; simulations by Mastin et al. [2024] suggesting that 90 wt.% of the total erupted mass consisted of entrained external water vapor in order to reproduce the observed max height (with an MER of $7 - 14 \times 10^7$ $\text{kg s}^{-1}$, see Supplementary Material Section S10).

The Fukutoku-Oka-no-Ba (FOB) eruption of August 13, 2021, was explosive and generated a 16 km (above sea level) water-rich plume while simultaneously creating a 0.1 $\text{km}^3$ pumice raft [Maeno et al. 2022; Chang et al. 2023; Fauria et

al. 2023]. It was estimated that the FOB had mass flux values of $10^5$–$10^7$ kg s$^{-1}$ [Maeno et al. 2022; Fauria et al. 2023].

Both eruptions exhibited partial collapse of the eruption column [Clare et al. 2023; Fauria et al. 2023; Kelly et al. 2024]. Partial collapse of the Hunga eruption column is thought to have generated devastating submarine volcaniclastic currents [Clare et al. 2023; Seabrook et al. 2023]. The raft from the FOB eruption is also suspected to have formed by near-field collapse of particles from the eruption column [Fauria et al. 2023]. Because 1-D models such as `Plumeria` do not simulate partial collapse, these recent eruptions, therefore, highlight one of the major limitations associated with the application of 1-D models. That said, the 1-D modeling results in Figure 2 make plain how external water can shift the column collapse condition in both directions (towards higher and lower MERs). In the case of Hunga 2022, one might envision the effects of external water on column collapse shifting through time as variable amounts of water may have been entrained above the vent.

## 5 Summary

We investigated the impact of external water on plume formation, height, and column collapse using `Plumeria`, a 1-D plume model. We conducted over 150,000 simulations where we varied MER, external water content, initial velocity, and initial magma temperature to understand how external water affected maximum column height and the column collapse condition. Our analysis included the examination of upward velocity, bulk mixture temperature, and bulk density at the vent, as well as their evolution along the column's vertical trajectory to clarify the mechanisms governing maximum column collapse. We show quantitatively that:

1. External water mainly affects column dynamics by shifting the column collapse condition.

2. Small to moderate amounts of external water (below $25 \pm 4$ wt.%) reduce the likelihood of column collapse in large mass flux eruptions by lowering the initial mixture density and enhancing buoyancy (Region 4). In contrast, external water contents above $25 \pm 4$ wt.% decrease net column temperature, promoting collapse and reducing maximum column height.

3. For low to moderate mass eruption rates ($\lesssim 10^6$ kg s$^{-1}$), external water has only a modest effect on plume height (Region 1), though reductions in plume height of up to ≈30 % occur at higher water fractions. For large mass eruption rates, the erupted mixture is too dense to become buoyant and thus plume height is unaffected by external water (Region 3).

4. Our results refine the classic view that Ri $\lesssim$ 1 defines the collapse threshold by showing that external water and magma temperature can shift the column collapse condition to lower Richardson numbers. Indeed, the MER at which column collapse occurs can vary by three orders of magnitude.

By conducting numerous simulations, we illuminate how the column collapse condition depends on water content, magma temperature, vent velocity, and mass flux. We show that the primary impact of external water is shifting the column collapse condition.

## Disclaimers

This product has been peer reviewed and approved for publication consistent with USGS Fundamental Science Practices (https://pubs.usgs.gov/circ/1367/).

## Author Contributions

The contributions of the authors to this work are as follows: Conceptualization was led by Kristen Fauria (KF) and Tushar Mittal (TM). Data curation and formal analysis were performed by Edgar Carrillo (EC), who also took charge of the investigation and visualization efforts. Funding acquisition was supported by EC and KF. The methodology was collaboratively developed by KF, EC, and TM. Project administration and resource provision were overseen by KF, who also served as the primary supervisor. The software development involved EC, TM, and Larry Mastin (LM), while validation efforts were conducted by EC and TM. EC was responsible for drafting the original manuscript, and all authors, EC, KF, TM, and LM, contributed to the review and editing of the final version.

## Acknowledgements

We thank Alexa Van Eaton for conversations that improved the content of this paper. We also thank Chiara Maria Petrone and Simona Scollo for their feedback. We thank Takehiro Koyaguchi, Mark Woodhouse, and two anonymous reviewers for comments on an earlier version of the manuscript. ELC acknowledges support from the Fisk Astronomy and Space Science Training (FASST) grant. TM acknowledges support from the Packard Fellowship for Science and Engineering.

## Data Availability

All the software used in this study is open-source and accessible through online repositories. The `Plumeria` software can be found at https://doi.org/10.5066/P1HVRKVN. `Python` scripts developed for data analysis and supplementary calculations are hosted on GitHub at https://github.com/elcarrillo/PlumeViz. Additionally, the simulation data supporting this study are available on Zenodo at https://doi.org/10.5281/zenodo.12510646.

## Copyright Notice



## References

Aubry, T. J., S. Engwell, C. Bonadonna, G. Carazzo, S. Scollo, A. R. Van Eaton, I. A. Taylor, D. Jessop, J. Eychenne, M. Gouhier, L. G. Mastin, K. L. Wallace, S. Biass, M. Bursik, R. G. Grainger, A. M. Jellinek, and A. Schmidt (2021). "The Independent Volcanic Eruption Source Parameter Archive (IVESPA, version 1.0): A new observational database to sup-

port explosive eruptive column model validation and development". *Journal of Volcanology and Geothermal Research* 417, page 107295. DOI: https://doi.org/10.1016/j.jvolgeores.2021.107295.

Cahalan, R. C. and J. Dufek (2021). "Explosive Submarine Eruptions: The Role of Condensable Gas Jets in Underwater Eruptions". *Journal of Geophysical Research: Solid Earth* 126(2), e2020JB020969. DOI: https://doi.org/10.1029/2020JB020969.

Carazzo, G., E. Kaminski, and S. Tait (2015). "The timing and intensity of column collapse during explosive volcanic eruptions". *Earth and Planetary Science Letters* 411, pages 208–217. DOI: https://doi.org/10.1016/j.epsl.2014.12.006.

Carey, S. and M. Bursik (2015). "Volcanic Plumes". *The Encyclopedia of Volcanoes*. Edited by H. Sigurdsson. Second Edition. Amsterdam: Academic Press. Chapter 32, pages 571–585. ISBN: 978-0-12-385938-9. DOI: https://doi.org/10.1016/B978-0-12-385938-9.00032-8.

Carr, J. L., Á. Horváth, D. L. Wu, and M. D. Friberg (2022). "Stereo Plume Height and Motion Retrievals for the Record-Setting Hunga Tonga-Hunga Ha'apai Eruption of 15 January 2022". *Geophysical Research Letters* 49(9). DOI: https://doi.org/10.1029/2022GL098131.

Chang, Y., I. McIntosh, T. Miyama, and Y. Miyazawa (2023). "Projection of August 2021 pumice dispersion from the Fukutoku Okanoba eruption in the western North Pacific". *Scientific Reports* 14(3945), pages 1444–1447. DOI: https://doi.org/10.1038/s41598-023-31058-0.

Clare, M. A., I. A. Yeo, S. Watson, R. Wysoczanski, S. Seabrook, K. Mackay, J. E. Hunt, E. Lane, P. J. Talling, E. Pope, S. Cronin, M. Ribó, T. Kula, D. Tappin, S. Henrys, C. de Ronde, M. Urlaub, S. Kutterolf, S. Fonua, S. Panuve, D. Veverka, R. Rapp, V. Kamalov, and M. Williams (2023). "Fast and destructive density currents created by ocean-entering volcanic eruptions". *Science* 381(6662), pages 1085–1092. DOI: 10.1126/science.adi3038.

Costa, A., Y. Suzuki, M. Cerminara, B. Devenish, T. E. Ongaro, M. Herzog, A. Van Eaton, L. Denby, M. Bursik, M. de'Michieli Vitturi, S. Engwell, A. Neri, S. Barsotti, A. Folch, G. Macedonio, F. Girault, G. Carazzo, S. Tait, E. Kaminski, L. Mastin, M. Woodhouse, J. Phillips, A. Hogg, W. Degruyter, and C. Bonadonna (2016). "Results of the eruptive column model inter-comparison study". *Journal of Volcanology and Geothermal Research* 326, pages 2–25. DOI: https://doi.org/10.1016/j.jvolgeores.2016.01.017.

Degruyter, W. and C. Bonadonna (2013). "Impact of wind on the condition for column collapse of volcanic plumes". *Earth and Planetary Science Letters* 377, pages 218–226. DOI: https://doi.org/10.1016/j.epsl.2013.06.041.

Fagents, S. A., T. K. P. Gregg, and R. M. C. Lopes (2012). *Modeling Volcanic Processes : The Physics and Mathematics of Volcanism*. Cambridge: Cambridge University Press. 421 pages. ISBN: 9781139021562. DOI: https://doi.org/10.1017/CBO9781139021562.

Fauria, K. E., M. Jutzeler, T. Mittal, A. K. Gupta, L. J. Kelly, J. Rausch, R. Bennartz, B. Delbridge, and L. Retailleau (2023). "Simultaneous creation of a large vapor plume and pumice raft by the 2021 Fukutoku-Oka-no-Ba shallow submarine eruption". *Earth and Planetary Science Letters* 609, page 118076. DOI: https://doi.org/10.1016/j.epsl.2023.118076.

Gupta, A. K., R. Bennartz, K. E. Fauria, and T. Mittal (2022). "Eruption chronology of the December 2021 to January 2022 Hunga Tonga-Hunga Ha'apai eruption sequence". *Communications Earth & Environment* 3(1), pages 1–10. DOI: https://doi.org/10.1038/s43247-022-00606-3.

Herzog, M., H.-F. Graf, C. Textor, and J. M. Oberhuber (1998). "The effect of phase changes of water on the development of volcanic plumes". *Journal of Volcanology and Geothermal Research* 87(1), pages 55–74. DOI: https://doi.org/10.1016/S0377-0273(98)00100-0.

Ichihara, M., P. D. Mininni, S. Ravichandran, C. Cimarelli, and C. Vagasky (2023). "Multiphase turbulent flow explains lightning rings in volcanic plumes". *Communications Earth & Environment* 4(1), page 417. DOI: 10.1038/s43247-023-01074-z.

Kaminski, É. and C. Jaupart (2001). "Marginal stability of atmospheric eruption columns and pyroclastic flow generation". *Journal of Geophysical Research: Solid Earth* 106(B10), pages 21785–21798. DOI: https://doi.org/10.1029/2001JB000215.

Kelly, L. J., K. E. Fauria, M. Manga, S. J. Cronin, F. H. Latu'ila, J. Paredes-Mariño, T. Mittal, and R. Bennartz (2024). "Airfall volume of the 15 January 2022 eruption of Hunga volcano estimated from ocean color changes". *Bulletin of Volcanology* 86(59). DOI: https://doi.org/10.1007/s00445-024-01744-6.

Koyaguchi, T. and Y. J. Suzuki (2018). "The Condition of Eruption Column Collapse: 1. A Reference Model Based on Analytical Solutions". *Journal of Geophysical Research: Solid Earth* 123(9), pages 7461–7482. DOI: https://doi.org/10.1029/2017JB015308.

Koyaguchi, T., Y. J. Suzuki, K. Takeda, and S. Inagawa (2018). "The Condition of Eruption Column Collapse: 2. Three-Dimensional Numerical Simulations of Eruption Column Dynamics". *Journal of Geophysical Research: Solid Earth* 123(9), pages 7483–7508. DOI: https://doi.org/10.1029/2017JB015259.

Koyaguchi, T. and A. W. Woods (1996). "On the formation of eruption columns following explosive mixing of magma and surface-water". *Journal of Geophysical Research* 101(B3), pages 5561–5574. DOI: https://doi.org/10.1029/95JB01687.

Maeno, F., T. Kaneko, M. Ichihara, Y. J. Suzuki, A. Yasuda, K. Nishida, and T. Ohminato (2022). "Seawater-magma interactions sustained the high column during the 2021 phreatomagmatic eruption of Fukutoku-Oka-no-Ba". *Communications Earth & Environment* 3(260). DOI: 10.1038/s43247-022-00594-4.

Mason, B. G., D. M. Pyle, and C. Oppenheimer (2004). "The size and frequency of the largest explosive eruptions on Earth". *Bulletin of Volcanology* 66(8), pages 735–748. DOI: 10.1007/s00445-004-0355-9.

Mastin, L. G., A. R. Van Eaton, and S. J. Cronin (2024). "Did steam boost the height and growth rate of the giant Hunga

eruption plume?" *Bulletin of Volcanology* 86(64). DOI: https://doi.org/10.1007/s00445-024-01749-1.

Mastin, L. G. (2007). "A user-friendly one-dimensional model for wet volcanic plumes". *Geochemistry, Geophysics, Geosystems* 8(3). DOI: 10.1029/2006GC001455.

– (2014). "Testing the accuracy of a 1-D volcanic plume model in estimating mass eruption rate". *Journal of Geophysical Research: Atmospheres* 119(5), pages 2474–2495. DOI: https://doi.org/10.1002/2013JD020604.

– (2024). *plumeria_wd software*. Software program.

Mastin, L. G., M. Guffanti, R. Servranckx, P. Webley, S. Barsotti, K. Dean, A. Durant, J. Ewert, A. Neri, W. Rose, D. Schneider, L. Siebert, B. Stunder, G. Swanson, A. Tupper, A. Volentik, and C. Waythomas (2009). "A multidisciplinary effort to assign realistic source parameters to models of volcanic ash-cloud transport and dispersion during eruptions". *Journal of Volcanology and Geothermal Research* 186(1), pages 10–21. DOI: https://doi.org/10.1016/j.jvolgeores.2009.01.008.

McCormick, M. P., L. W. Thomason, and C. R. Trepte (1995). "Atmospheric Effects of the Mt Pinatubo Eruption". *Nature* 373(6513), pages 399–404. DOI: https://doi.org/10.1038/373399a0.

Morton, B. R., G. Taylor, F. R. S, and J. S. Turner (1956). "Turbulent gravitational convection from maintained and instantaneous sources". *Proceedings of the Royal Society of London. Series A. Mathematical and Physical Sciences* 234(1196), pages 1–23. DOI: https://doi.org/10.1098/rspa.1956.0011.

Proud, S. R., A. T. Prata, and S. Schmauss (2022). "The January 2022 eruption of Hunga Tonga-Hunga Ha'apai volcano reached the mesosphere". *Science* 378(6619), pages 554–557. DOI: 10.1126/science.abo4076.

Rowell, C. R., A. M. Jellinek, S. Hajimirza, and T. J. Aubry (2022). "External Surface Water Influence on Explosive Eruption Dynamics, With Implications for Stratospheric Sulfur Delivery and Volcano-Climate Feedback". *Frontiers in Earth Science* 10. DOI: 10.3389/feart.2022.788294.

Seabrook, S., K. Mackay, S. J. Watson, M. A. Clare, J. E. Hunt, I. A. Yeo, E. M. Lane, M. R. Clark, R. Wysoczanski, A. A. Rowden, T. Kula, L. J. Hoffmann, E. Armstrong, and M. J. M. Williams (2023). "Volcaniclastic density currents explain widespread and diverse seafloor impacts of the 2022 Hunga Volcano eruption". *Nature Communications* 14(1), page 7881. DOI: 10.1038/s41467-023-43607-2.

Sheridan, M. F. and K. H. Wohletz (1983). "Hydrovolcanism: basic considerations and review". *Journal of Volcanology and Geothermal Research* 17(1-4), pages 1–29. DOI: https://doi.org/10.1016/0377-0273(83)90060-4.

Sparks, R. S. J. and L. Wilson (1976). "A model for the formation of ignimbrite by gravitational column collapse". *Journal of the Geological Society* 132(4), pages 441–451. DOI: https://doi.org/10.1144/gsjgs.132.4.0441.

Sparks, R., M. Bursik, S. Carey, J. Gilbert, L. Glaze, H. Sigurdsson, and A. Woods (1997). *Volcanic plumes*. Wiley, pages 100–120. ISBN: 0471939013.

Suzuki, Y. J., A. Costa, M. Cerminara, T. Esposti Ongaro, M. Herzog, A. R. Van Eaton, and L. C. Denby (2016). "Inter-comparison of three-dimensional models of volcanic plumes". *Journal of Volcanology and Geothermal Research* 326, pages 26–42. DOI: https://doi.org/10.1016/j.jvolgeores.2016.06.011.

Suzuki, Y. J. and T. Koyaguchi (2012). "3-D numerical simulations of eruption column collapse: Effects of vent size on pressure-balanced jet/plumes". *Journal of Volcanology and Geothermal Research* 221-222, pages 1–13. DOI: https://doi.org/10.1016/j.jvolgeores.2012.01.013.

Trolese, M., M. Cerminara, T. Esposti Ongaro, and G. Giordano (2019). "The footprint of column collapse regimes on pyroclastic flow temperatures and plume heights". *Nature Communications* 10(1), page 2476. DOI: 10.1038/s41467-019-10337-3.

Valentine, G. A. and K. H. Wohletz (1989). "Numerical models of Plinian eruption columns and pyroclastic flows". *Journal of Geophysical Research: Solid Earth* 94(B2), pages 1867–1887. DOI: https://doi.org/10.1029/JB094iB02p01867.

Van Eaton, A. R., M. Herzog, C. J. N. Wilson, and J. McGregor (2012a). "Ascent dynamics of large phreatomagmatic eruption clouds: The role of microphysics". *Journal of Geophysical Research: Solid Earth* 117(B3). DOI: https://doi.org/10.1029/2011JB008892.

Van Eaton, A. R., J. Lapierre, S. A. Behnke, C. Vagasky, C. J. Schultz, M. Pavolonis, K. Bedka, and K. Khlopenkov (2023). "Lightning Rings and Gravity Waves: Insights Into the Giant Eruption Plume From Tonga's Hunga Volcano on 15 January 2022". *Geophysical Research Letters* 50(12). DOI: https://doi.org/10.1029/2022GL102341.

Van Eaton, A. R., J. D. Muirhead, C. J. N. Wilson, and C. Cimarelli (2012b). "Growth of volcanic ash aggregates in the presence of liquid water and ice: an experimental approach". *Bulletin of Volcanology* 74(9), pages 1963–1984. DOI: 10.1007/s00445-012-0634-9.

Vömel, H., S. Evan, and M. Tully (2022). "Water vapor injection into the stratosphere by Hunga Tonga-Hunga Ha'apai". *Science* 377(6613), pages 1444–1447. DOI: 10.1126/science.abq2299.

White, J. D., J. L. Smellie, and D. A. Clague (2003). *Explosive Subaqueous Volcanism*. Geophysical monograph 140. Washington, D.C: American Geophysical Union. ISBN: 087590999X.

Wohletz, K. H. (1986). "Explosive magma-water interactions: Thermodynamics, explosion mechanisms, and field studies". *Bulletin of Volcanology* 48, pages 245–264. DOI: https://doi.org/10.1007/BF01081754.

Woods, A. (1988). "The fluid dynamics and thermodynamics of eruption columns". *Bulletin of Volcanology* 50(169-193), pages 1444–1447. DOI: https://doi.org/10.1007/BF01079681.

Woods, A. W. and C.-C. P. Caulfield (1992). "A laboratory study of explosive volcanic eruptions". *Journal of Geophysical Research: Solid Earth* 97(B5), pages 6699–6712. DOI: https://doi.org/10.1029/92JB00176.

Woods, A. W. (1995). "The dynamics of explosive volcanic eruptions". *Reviews of Geophysics* 33(4), pages 495–530. DOI: https://doi.org/10.1029/95RG02096.

Xu, J., D. Li, Z. Bai, M. Tao, and J. Bian (2022). "Large Amounts of Water Vapor Were Injected into the Stratosphere by the Hunga Tonga Hunga Haapai Volcano Eruption". *Atmosphere* 13(6). DOI: 10.3390/atmos13060912.